

Synthesis and Characterization of Optically Active and Racemic Forms of Cyclometalated Rh(III) Complexes. An Experimental and Theoretical Emission Study

Liana Ghizdavu, Olivier Lentzen, Stephan Schumm, André Brodkorb, Cécile Moucheron, and Andrée Kirsch-De Mesmaeker*

Organic Chemistry and Photochemistry, Free University of Brussels, CP: 160/08, 50 avenue Franklin Roosevelt, 1050 Brussels, Belgium

Received July 3, 2002

The optically active cyclometalated Rh(III) complexes, Δ [Rh(thpy4,5p(*R,R*)py)₂TAP]Cl, Λ [Rh(thpy4,5p(*S,S*)py)₂TAP]Cl, and Δ [Rh(phpy4,5p(*R,R*)py)₂TAP]Cl (where TAP = 1,4,5,8-tetraazaphenanthrene, thpy4,5p(*R,R*)py = (8*R*,10*R*)-2-(2'-thienyl)-4,5-pinenopyridine and phpy4,5p(*R,R*)py = (8*R*,10*R*)-2-(2'-phenyl)-4,5-pinenopyridine) have been prepared and characterized. Their photophysics has been examined in parallel with that of rac[Rh(thpy)₂TAP]Cl and rac[Rh(phpy)₂TAP]Cl. Their behaviors have been rationalized from results of TD-DFT calculations. The complexes with thienylpyridine (thpy) as cyclometalating ligands exhibit ³CT (from thpy to TAP) and ³LC_{π-π*} (centered on thpy) emissions in a solvent matrix at 77 K and one ³CT luminescence at room temperature. In contrast, with phenylpyridine (phpy), the complexes show only one ³CT emission (from phpy to TAP) at both temperatures.

Introduction

The interest in enantiomerically pure metallic compounds has rapidly increased during this past decade in several research areas such as bioinorganic and supramolecular chemistry and catalysis. Inorganic stereochemistry has been the subject of recent reviews.^{1–3} This increasing need for optically pure metallic complexes originates from their specific interaction with other stereoactive partners and the fact that intermolecular or intramolecular elementary processes such as energy or electron transfers depend on the stereoisomers.^{1,4} More specifically, the important role played by the chirality of octahedral complexes when used as photoprobes and photoreagents of DNA has been demonstrated.^{4–6} As the stereoisomers can exhibit different affinities and geometries of interaction with DNA, different rates of

electron or energy transfers can be obtained. Until recently, the search for new luminescent inorganic compounds, reporters of DNA structures, has been limited mainly to optically pure Ru^{II} complexes. Less attention has been devoted to Ir^{III} and Rh^{III} polypyridyl complexes and their cyclometalated compounds.^{5,7–12} In this work, we present the synthesis and photophysical characterization of new optically active cyclometalated Rh(III) complexes that could become possible DNA sensors with comparison to the similar racemic compounds. TD-DFT calculations have been carried out to rationalize the emission behaviors. We choose the stereoselective synthesis developed by von Zelewsky and co-workers for the preparation of the optically active compounds.^{2,13,14} Stereoselective synthesis appears indeed to be one of the most promising approaches for the development

* To whom correspondence should be addressed. E-mail: akirsch@ulb.ac.be. Fax: +3226503606.

- (1) Keene, F. R. *Coord. Chem. Rev.* **1997**, *166*, 121–159.
- (2) Knof, U.; von Zelewsky, A. *Angew. Chem., Int. Ed.* **1999**, *38*, 302–322.
- (3) von Zelewsky, A.; Mamula, O. *J. Chem. Soc., Dalton Trans* **2000**, *3*, 219–231.
- (4) Brodkorb, A.; Kirsch-De Mesmaeker, A.; Rutherford, T. J.; Keene, F. R. *Eur. J. Inorg. Chem.* **2001**, 2151–2160.
- (5) Erkkila, K. E.; Odom, D. T.; Barton, J. K. *Chem. Rev.* **1999**, *99*, 2777–2795.
- (6) Pyle, A. M.; Morii, T.; Barton, J. K. *J. Am. Chem. Soc.* **1990**, *112*, 9432–9434.

- (7) Pyle, A. M.; Barton, J. K. *Prog. Inorg. Chem.* **1990**, *38*, 413–475.
- (8) Moucheron, C.; Kirsch-De Mesmaeker, A.; Kelly, J. M. *J. Photochem. Photobiol., B* **1997**, *40*, 91–106.
- (9) Kirsch-De Mesmaeker, A.; Lecomte, J.-P.; Kelly, J. M. *Topics in Current Chemistry: Electron Transfer II*; Springer Verlag: New York, 1996; Vol. 177.
- (10) Didier, P.; Ortman, I.; Kirsch-De Mesmaeker, A.; Watts, R. J. *Inorg. Chem.* **1993**, *32*, 5239–5245.
- (11) Maestri, M.; Balzani, V.; Deuschel-Cornioley, C.; von Zelewsky, A. *Advances in Photochemistry*; John Wiley & Sons: New York, 1992; Vol. 17.
- (12) Kisko, J. L.; Barton, J. K. *Inorg. Chem.* **2000**, *39*, 4942–4949.
- (13) Ghizdavu, L.; Kolp, B.; von Zelewsky, A.; Stoeckli-Evans, H. *Eur. J. Inorg. Chem.* **1999**, *8*, 1271–1279.

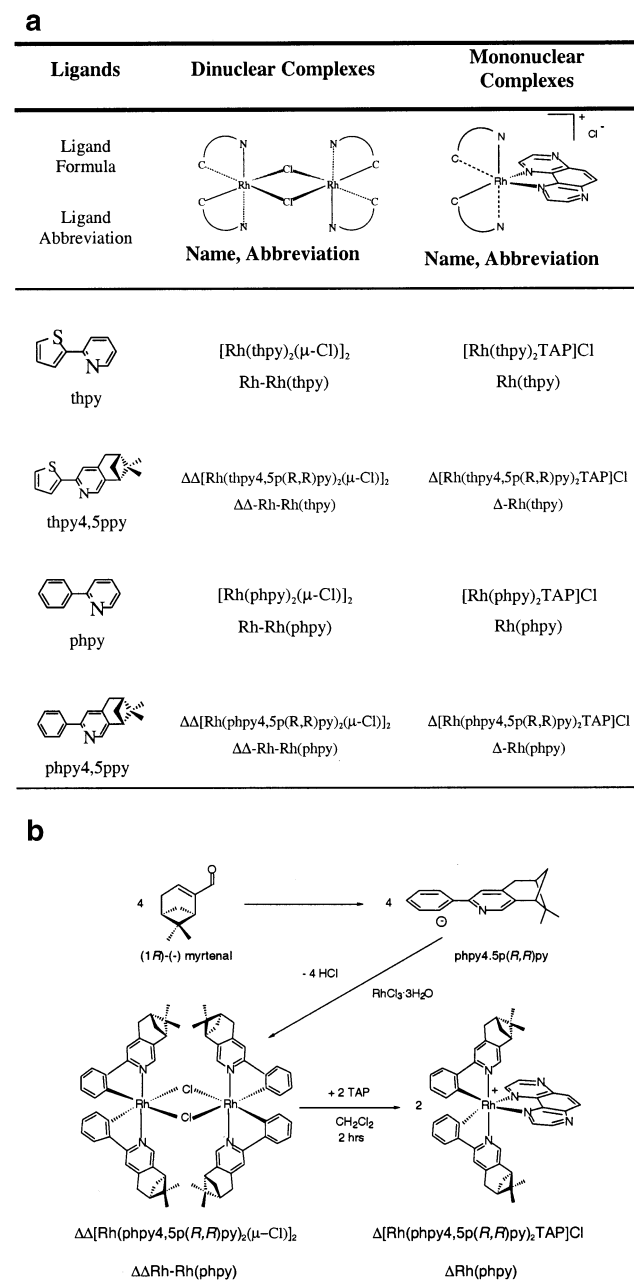
of optically pure complexes. According to this method, the chirality at the metal center (Δ or Λ) is controlled by the choice of the enantiomerically pure chiral bidentate ligands that are used. Available natural products such as (–)-myrtenal and (+)- α -pinene can easily be used to synthesize chiral, bidentate cyclometalating (C \wedge N) ligands, such as 2,2'-phenyl-4,5-(*R,R*)-pinenopyridine. Cyclometalation of this ligand is a highly regioselective reaction reducing drastically the number of possible isomers. As shown in the literature, due to the trans influence, only C,C-cis isomers are obtained.^{11,13,15} Therefore, the pinenes in the trans position, due to steric hindrances, lead during the formation of the dinuclear complexes $[\text{Rh}(\text{C}\wedge\text{N})_2(\mu\text{-Cl})_2]$ to homochiral ($\Delta\Delta$ or $\Lambda\Lambda$) compounds (Scheme 1a,b).¹³ Upon cleavage of the μ -dichloro bridge of these dimers with bidentate ligands, mononuclear complexes are obtained. It has been shown that this type of cleavage reaction occurs under retention of configuration.¹⁴

Previous luminescence studies^{10,11,16,17} showed that the photophysics of Rh^{III} cyclometalated complexes could be quite different from that of the Ru^{II} polypyridyl compounds. A tuning of the excited state properties could be obtained by the choice of the noncyclometalating ligand (bpy vs TAP).¹⁰ For example, it was shown^{10,16,17} that the emission of $[\text{Rh}(\text{phpy})_2\text{bpy}]\text{Cl}$ is very weak at room temperature and originates at 77 K from a ³LC excited state whereas the complexes containing strong π -deficient ligands such as TAP or HAT (HAT = 1,4,5,8,9,12-hexaazatriphenylene) in $[\text{Rh}(\text{phpy})_2\text{TAP}]\text{Cl}$ or $[\text{Rh}(\text{phpy})_2\text{HAT}]\text{Cl}$ emit from ³CT excited states at 77 K and at room temperature. Therefore, on the basis of these previous photophysical results^{10,11,16,17} and motivated by the potential interest of chirally pure Rh(III) complexes as DNA photoprobes, we have decided to use the TAP ligand for the new chiral cyclometalated Rh(III) complexes: $\Delta[\text{Rh}(\text{thpy}4,5\text{p}(\text{R},\text{R})\text{py})_2\text{TAP}]\text{Cl}$, $\Lambda[\text{Rh}(\text{thpy}4,5\text{p}(\text{S},\text{S})\text{py})_2\text{TAP}]\text{Cl}$, and $\Delta[\text{Rh}(\text{phpy}4,5\text{p}(\text{R},\text{R})\text{py})_2\text{TAP}]\text{Cl}$ (Scheme 1a,b). In this paper, we thus present the synthesis, characterization, and study of the photophysical properties of these complexes from an experimental and theoretical point of view. For the sake of comparison, we have also included the non-pinene-substituted compounds $[\text{Rh}(\text{thpy})_2\text{TAP}]\text{Cl}$ as well as the already reported $[\text{Rh}(\text{phpy})_2\text{TAP}]\text{Cl}$ (Scheme 1a,b).¹⁰

Experimental Section

Materials. Unless otherwise stated, all chemicals and reagents were obtained from Fluka, Aldrich, Merck, or Lancaster and used without further purification. (1*R*)-(-)-Myrtenal was obtained from Aldrich, >98%, $[\alpha]_{\text{D}}^{20} -14.6^\circ$, while the ligands, 2-(2'-phenyl)-pyridine and 2-(2'-thienyl)-pyridine, were purchased from Merck and Lancaster, respectively. The complexes $[\text{Rh}(\text{phpy})_2(\mu\text{-Cl})_2]$ ¹⁵

Scheme 1



(Rh–Rh(phpy)) and $[\text{Rh}(\text{phpy})_2(\text{TAP})]\text{Cl}$ ¹⁰ have been previously synthesized. The photophysical behavior of $[\text{Rh}(\text{phpy})_2(\mu\text{-Cl})_2]$ ¹⁵ has already been reported in the literature, but additional measurements had to be carried out for the mononuclear complex $[\text{Rh}(\text{phpy})_2(\text{TAP})]\text{Cl}$ (see Results and Discussion).

Instrumentation. ¹H NMR (300 MHz) and ¹³C NMR (75.46 MHz) spectra were obtained on a Bruker Avance-300 instrument. The ESMS (electrospray mass spectrometry) spectra were measured on a VG BioQ mass spectrometer, and the EI (electronic impact) spectrum was measured on an Autospec (Fisons) mass spectrometer. UV–vis spectra were recorded using a Hewlett-Packard 8452 UV–vis diode array spectrophotometer [λ_{max} in nm, ϵ in $\text{M}^{-1} \text{cm}^{-1}$], and CD spectra were recorded on a JASCO J-710 spectropolarimeter [λ_{max} , ($\Delta\epsilon$) in nm]. Emission spectra were recorded using a Shimadzu RF-5001 PC spectrofluorimeter. The excitation source was a 150 W xenon lamp. Low temperature emission lifetimes and luminescence spectra were obtained using an Oxford Instruments

(14) Ghizdavu, L.; von Zelewsky, A.; Stoeckli-Evans, H. *Eur. J. Inorg. Chem.* **2001**, 4, 993–1003.

(15) Sprouse, S.; King, K. A.; Spellane, P. J.; Watts, R. J. *J. Am. Chem. Soc.* **1984**, 106, 6647–6653.

(16) Maestri, M.; Sandrini, D.; Balzani, V.; Maeder, U.; von Zelewsky, A. *Inorg. Chem.* **1987**, 26, 1323–1327.

(17) Ohsawa, Y.; Sprouse, S.; King, K. A.; De Armond, M. K.; Hanck, K. W.; Watts, R. J. *J. Phys. Chem.* **1987**, 91, 1047–1054.

DN 1704 nitrogen cryostat controlled by an Oxford Instruments Intelligent Temperature Controller (ITC 4). The transient signal was detected by a modified Applied Photophysics laser kinetic spectrometer equipped with a monochromator (Applied Photophysics f/3.4) and a red sensitive Hamamatsu R928 photomultiplier tube connected to an oscilloscope HP 5248. A harmonic wavelength of the pulsed Nd:YAG laser was used as the excitation source (Continuum NY 61-10, $\lambda_{\text{exc}} = 355$ nm; 10 mJ per pulse). The data were transferred to a PC to obtain the lifetimes.

An SPC Edinburgh Instruments FL-900 spectrofluorimeter equipped with a nitrogen-filled discharge lamp and a peltier-cooled Hamamatsu R928 PM tube was used for the room temperature lifetime measurements. The emission decays were analyzed with the Edinburgh Instruments software (version 3.0).

(8R,10R)-2-(2'-Phenyl)-4,5-pinenopyridine. Under stirring, ammonium acetate (2.46 g, 34.28 mmol) was dissolved in a solution of (1-phenacyl)pyridinium bromide¹⁸ (4.76 g, 17.11 mmol) in formamide (20 mL), and the resulting yellowish solution was heated at 50 °C for 30 min. (-)-Myrtenal (2.60 g, 17.31 mmol) was added dropwise over a 10 min period producing a change in color from yellow to orange. The reaction mixture, refluxed at 60 °C for 16 h, was quenched by addition of water (20 mL), and the brownish solution was extracted with (8 × 100 mL) hexane. After drying over MgSO₄, the solvent was removed, and orange crystals were yielded at 4 °C. Yield: 72% (3.07 g). ¹H NMR (CDCl₃, 300 MHz, δ (ppm), J (Hz)): 8.2 (s, 1H, H-C(6)); 7.94 (dd, 2H, ³ $J = 8.35$, ⁴ $J = 1.4$, H-C(2')); 7.5 (s, 1H, H-C(3)); 7.46–7.32 (m, 3H, H-C(3',4')); 3.01 (d, 2H, ³ $J = 2.5$, H-C(7)); 2.84 (dd, 1H, ⁴ $J = 5.5$, ³ $J = 5.5$, H-C(10)); 2.7 (ddd, 1H, ² $J = 9.5$, ³ $J = 5.7$, ³ $J = 5.7$, H-C(9 exo)); 2.30 (tdd, 1H, ⁴ $J = 5.5$, ³ $J = 5.5$, ³ $J = 2.8$, H-C(8)); 1.41 (s, 3H, H-C(13)); 1.23 (d, 2H, ² $J = 9.5$, H-C(9 endo)); 0.65 (s, 3H, H-C(12)). ¹³C NMR (CDCl₃, 75 MHz, δ (ppm)): 156.1, 146.3, 145.6, 141.6, 140.3, 129.0, 128.8, 127.1, 120.4, 44.8, 40.5, 39.8, 33.3, 32.3, 26.5, 21.9. MS (EI) m/z : 249 (28, M⁺), 234 (23, M⁺ - CH₃), 220 (6, M⁺ - C₂H₅), 206 (100, M⁺ - C₃H₇), 193 (11, M⁺ - C₄H₈), 178 (10, M⁺ - C₅H₁₁), 128 (10, M⁺ - C₉H₁₃). UV-vis (λ (nm), ϵ (M⁻¹ cm⁻¹) (EtOH/MeOH 4:1)): 281 (10200), 252 (15700) (not soluble in CH₃CN).

[Rh(phpy4,5p(R,R)py)₂(μ -Cl)]₂. Using a modified literature procedure,¹⁵ a mixture of RhCl₃·3H₂O (264 mg, 1 mmol) and phpy4,5p(R,R)py (748 mg, 3 mmol) was suspended in 10 mL of glycerol and dispersed during 3 min in an ultrasonic bath. The resulting solution was heated at 150 °C and refluxed for 24 h. After cooling to room temperature, the reaction mixture was quenched by addition of HCl (30 mL, 1 M) and refrigerated overnight. The brownish precipitate was filtered off and washed with HCl (75 mL, 1 M) and MeOH (60 mL). The remaining precipitate was dissolved in 50 mL of CH₂Cl₂ and filtered. The orange filtrate was evaporated, and the orange powder was dried in vacuo. The ratio of the two diastereomers formed ($\Delta\Delta$ [Rh(phpy4,5p(R,R)py)₂(μ -Cl)]₂/ $\Delta\Delta$ [Rh(phpy4,5p(R,R)py)₂(μ -Cl)]₂) was calculated from the signal intensity of the protons at the 6 position in the ¹H NMR spectra. A ratio $\Delta\Delta$ [Rh(phpy4,5p(R,R)py)₂(μ -Cl)]₂/ $\Delta\Delta$ [Rh(phpy4,5p(R,R)py)₂(μ -Cl)]₂ of 4:1 was observed. The purification and separation of the different diastereoisomers was carried out by preparative thin layer plate silica chromatography with CH₃CN/BuOH/H₂O/KNO₃ (4:1:1:0.1) as eluent. Another product, Δ [Rh(phpy4,5p(R,R)py)₂(NO₃)], was isolated after purification by chromatography. This mononuclear complex was obtained through the replacement of the chloride bridge by NO₃⁻ used in the eluent during chromatography. The yield after the second separation was 27% ($\Delta\Delta$), 12% (Δ).

$\Delta\Delta$ [Rh(phpy4,5p(R,R)py)₂(μ -Cl)]₂. Yield (separation): 70 mg (79%). TLC: silica gel, CH₃CN/BuOH/H₂O/KNO₃ 4:1:1:0.1. ¹H NMR (CD₃CN, 300 MHz, δ (ppm), J (Hz)): 8.94 (s, 4H, H-C(6)); 7.77 (s, 4H, H-C(3)); 7.53 (dd, 4H, ³ $J = 7.54$, ⁴ $J = 1.4$, H-C(6')); 6.79 (ddd, 4H, ³ $J = 7.54$, ³ $J = 6.6$, ⁴ $J = 1.0$, H-C(5')); 6.64 (ddd, 4H, ³ $J = 7.82$, ³ $J = 6.6$, ⁴ $J = 1.4$, H-C(4')); 6.07 (dd, 4H, ³ $J = 7.7$, ⁴ $J = 1.4$, H-C(3')); 3.17 (d, 8H, ³ $J = 2.0$, H-C(7)); 3.01 (dd, 4H, ⁴ $J = 5.5$, ³ $J = 5.5$, H-C(10)); 2.78 (ddd, 4H, ² $J = 9.7$, ³ $J = 5.8$, ³ $J = 5.8$, H-C(9exo)); 2.37 (tdd, 4H, ⁴ $J = 5.5$, ³ $J = 5.5$, ³ $J = 2.74$, H-C(8)); 1.46 (s, 12H, H-C(13)); 1.32 (d, 4H, ² $J = 9.6$, H-C(9endo)); 0.81 (s, 12H, H-C(12)). MS (electrospray) m/z : 1233 (10, M⁺ - Cl⁻), 634 (100, Rh(phpy4,5p(R,R)py)₂Cl + 6H⁺), 599 (4, Rh(phpy4,5p(R,R)py)₂). UV-vis (λ (nm), ϵ (M⁻¹ cm⁻¹)) (CH₃CN): 357 (12500), 300 (sh), 266 (57700), 237 (sh). CD (λ (nm), $\Delta\epsilon$) (CH₃CN): 369 (6.6), 333 (-7.8), 313 (-6.9), 286 (5.9), 252 (-).

Δ [Rh(phpy4,5p(R,R)py)₂](NO₃). Yield (separation): 15 mg (17%). TLC: silica gel, CH₃CN/BuOH/H₂O/KNO₃ 4:1:1:0.1. ¹H NMR (CD₃CN, 300 MHz, δ (ppm), J (Hz)): 8.47 (s, 4H, H-C(6)); 7.88 (s, 4H, H-C(3)); 7.61 (dd, 4H, ³ $J = 7.68$ Hz, ⁴ $J = 1.37$ Hz, H-C(6')); 6.90 (ddd, 4H, ³ $J = 7.54$, ³ $J = 6.44$, ⁴ $J = 1.10$, H-C(5')); 6.72 (ddd, 4H, ³ $J = 7.54$, ³ $J = 6.44$, ⁴ $J = 1.37$, H-C(4')); 6.02 (dd, 4H, ³ $J = 7.68$, ⁴ $J = 1.1$, H-C(3')); 3.22 (d, 8H, ³ $J = 2.2$, H-C(7)); 3.06 (dd, 4H, ⁴ $J = 5.5$, ³ $J = 5.21$, H-C(10)); 2.82 (ddd, 4H, ² $J = 9.7$, ³ $J = 5.8$, ³ $J = 5.8$, H-C(9exo)); 2.42 (tdd, 4H, ⁴ $J = 5.5$, ³ $J = 5.8$, ³ $J = 2.6$, H-C(8)); 1.47 (s, 12H, H-C(13)); 1.32 (d, 4H, ² $J = 9.6$, H-C(9endo)); 0.81 (s, 12H, H-C(12)). MS (electrospray) m/z : 599 (100, Rh(phpy4,5p(R,R)py)₂). UV-vis (λ (nm), ϵ (M⁻¹ cm⁻¹)) (CH₃CN): 357 (7300), 300 (sh), 266 (21800), 237 (sh). CD (λ (nm), $\Delta\epsilon$) (CH₃CN): 369 (4.2), 333 (-7.6), 323 (-7.6), 279 (13.3), 252 (-18.3).

Δ [Rh(phpy4,5p(R,R)py)₂(TAP)]Cl. A solution of $\Delta\Delta$ [Rh(phpy4,5p(R,R)py)₂(μ -Cl)]₂ (63.51 mg, 0.05 mmol) and 1,4,5,8-tetraazaphenanthrene (TAP) (18.22 mg, 0.1 mmol) in 20 mL of CH₂Cl₂ was refluxed 2 h under N₂ and protected from the light. The solvent was evaporated, and the pale yellow powder of Δ -[Rh(phpy4,5p(R,R)py)₂(TAP)]Cl was dried in vacuo. Further purification was carried out by preparative thin layer plate silica chromatography with EtOH/NaCl (20:1) as eluent. Yield: 31.06 mg (76%).

A second method, starting from Δ [Rh(phpy4,5p(R,R)py)₂](NO₃) that was yielded as a byproduct during the preparation of [Rh(phpy4,5p(R,R)py)₂(μ -Cl)]₂, was used to prepare the TAP complex by refluxing Δ [Rh(phpy4,5p(R,R)py)₂](NO₃) (10.00 mg, 0.015 mmol) and TAP (2.87 mg, 0.015 mmol) in 10 mL of CH₂Cl₂ during 90 min under N₂ and protection from light. It was treated as already described for the dimer cleavage. Yield: 9.84 mg (80%).

¹H NMR (CD₃CN, 300 MHz, δ (ppm), J (Hz)): 9.22 (d, 2H, ³ $J = 2.2$, H-C(2'', 7'')); 8.57 (s, 4H, H-C(9'', 10'')); 8.3 (d, 2H, ³ $J = 2.2$, H-C(3'', 6'')); 7.88 (s, 2H, H-C(3)); 7.81 (dd, 2H, ³ $J = 7.68$, ⁴ $J = 1.37$, H-C(6'')); 7.12 (ddd, 2H, ³ $J = 7.54$, ³ $J = 6.32$, ⁴ $J = 1.4$, H-C(5'')); 6.96 (ddd, 2H, ³ $J = 7.54$, ³ $J = 6.32$, ⁴ $J = 1.4$, H-C(4'')); 6.91 (s, 2H, H-C(6)); 6.32 (dd, 2H, ³ $J = 7.68$, ⁴ $J = 1.1$, H-C(3'')); 3.06 (d, 4H, ³ $J = 2.7$, H-C(7)); 2.47–2.24 (m, 4H, H-C(10), H-C(9exo)); 2.22 (tdd, 2H, ⁴ $J = 5.5$, ³ $J = 5.5$, ³ $J = 2.74$, H-C(8)); 1.28 (s, 6H, H-C(13)); 0.83 (d, 2H, ² $J = 9.33$, H-C(9endo)); 0.69 (s, 6H, H-C(12)). MS (electrospray) m/z : 781 (100, M - Cl⁻), 681 (3, M⁺ - C₇H₁₆), 640 (5, M⁺ - C₁₀H₂₁). UV-vis (λ (nm), ϵ (M⁻¹ cm⁻¹)) (CH₃CN): 357 (10900), 283 (sh), 268 (33900). CD (λ (nm), $\Delta\epsilon$) (CH₃CN): 367 (13), 332 (-11.1), 306 (-18.5), 270 (10.8), 246 (-11.6).

Δ [Rh(thpy4,5p(R,R)py)₂(TAP)]Cl. A solution of $\Delta\Delta$ [Rh(thpy4,5p(R,R)py)₂(μ -Cl)]₂¹³ (15.00 mg, 0.012 mmol) and TAP

(18) Collomb, P.; Von Zelewsky, A. *Tetrahedron: Asymmetry* **1995**, *6*, 2903–2904.

(4.22 mg, 0.023 mmol) in 15 mL of CH_2Cl_2 was refluxed for 1 h 30 min under N_2 and protected from light. The solvent was evaporated and an orange powder of $\Delta[\text{Rh}(\text{thpy}4,5\text{p}(\text{R},\text{R})\text{py})_2(\text{TAP})]\text{Cl}$ was obtained. The orange product was dissolved in 3 mL of CH_2Cl_2 , reprecipitated with diethyl ether by slow diffusion, collected and dried *in vacuo*. Yield: 17 mg (86%) of orange $\Delta[\text{Rh}(\text{thpy}4,5\text{p}(\text{R},\text{R})\text{py})_2(\text{TAP})]\text{Cl}$. Further purification was carried out by preparative thin-layer chromatography on silica with EtOH/NaCl (NaCl saturated water solution) (20:1) as eluent. ^1H NMR (CD_3CN , 300 MHz, δ (ppm), J (Hz)): 9.26 (d, 2H, $^3J = 2.5$, H-C(2'', 7'')); 8.58 (s, 2H, H-C(9'', 10'')); 8.31 (d, 2H, $^3J = 2.2$, H-C(3'', 6'')); 7.49 (d, 2H, $^3J = 4.7$, H-C(5'')); 7.45 (s, 2H, H-C(3)); 6.88 (s, 2H, H-C(6)) 6.31 (d, 2H, $^3J = 4.7$, H-C(4')); 3.01 (d, 4H, $^3J = 2.7$, H-C(7)); 2.45–2.16 (m, 6H, H-C(10), H-C(9_{exo}), H-C(8)); 1.27 (s, 6H, H-C(13)); 0.81 (d, 2H, $^2J = 9.05$, H-C(9_{endo})); 0.67 (s, 6H, H-C(12)). MS (electrospray) m/z : 793 (100, $\text{M} - \text{Cl}^-$). UV-vis (λ (nm), ϵ ($\text{M}^{-1} \text{cm}^{-1}$)) (CH_3CN): 375 (11800), 322 (sh), 284 (35900). CD (λ (nm), $\Delta\epsilon$) (CH_3CN): 387 (14.0), 353 (-12.5), 298 (-12.4), 269 (0.35), 249 (-1.4.), 215 (-4.6).

$\Delta[\text{Rh}(\text{thpy}4,5\text{p}(\text{S},\text{S})\text{py})_2(\text{TAP})]\text{Cl}$. This compound was synthesized from $\Delta\Delta[\text{Rh}(\text{thpy}4,5\text{p}(\text{S},\text{S})\text{py})_2(\mu\text{-Cl})]_2$ ¹³ using the method described for $\Delta[\text{Rh}(\text{thpy}4,5\text{p}(\text{R},\text{R})\text{py})_2(\text{TAP})]\text{Cl}$. All the data are identical to those of $\Delta[\text{Rh}(\text{thpy}4,5\text{p}(\text{R},\text{R})\text{py})_2(\text{TAP})]\text{Cl}$ except that the CD spectrum is the mirror image of the $\Delta[\text{Rh}(\text{thpy}4,5\text{p}(\text{S},\text{S})\text{py})_2(\text{TAP})]\text{Cl}$ enantiomer (Figure 3).

$[\text{Rh}(\text{thpy})_2(\text{TAP})]\text{Cl}$. This complex was prepared as described for $\Delta[\text{Rh}(\text{thpy}4,5\text{p}(\text{R},\text{R})\text{py})_2(\text{TAP})]\text{Cl}$, using $[\text{Rh}(\text{thpy})_2(\mu\text{-Cl})]_2$ ¹⁹ (35 mg, 0.04 mmol) and TAP (14 mg, 0.08 mmol) in 15 mL of CH_2Cl_2 . After purification by preparative thin layer plate silica chromatography with EtOH/NaCl saturated aqueous solution (20:1) as eluent, and with CH_3COOEt as solvent for desorption of the complex from silica, an orange crystalline material was obtained by slow diffusion of diethyl ether into a CH_2Cl_2 solution of $[\text{Rh}(\text{thpy})_2(\text{TAP})]\text{Cl}$. Yield: 29.4 mg (60%). ^1H NMR (CD_3CN , 300 MHz, δ (ppm), J (Hz)): 9.89 (d, 2H, $^3J = 2.5$, H-C(2'', 7'')); 8.61 (s, 2H, H-C(9'', 10'')); 8.34 (d, 2H, $^3J = 2.2$, H-C(3'', 6'')); 7.80 (ddd, 2H, $^3J = 7.6$, $^3J = 7.7$, $^4J = 1.4$, H-C(4)); 7.65 (d, 2H, $^3J = 7.68$, H-C(3)); 7.61 (d, 2H, $^3J = 4.9$, H-C(5'')); 6.42 (ddd, 2H, $^3J = 5.6$, $^4J = 1.1$, $^4J = 1.4$, H-C(6)); 6.79 (ddd, 2H, $^3J = 7.41$, $^3J = 7.41$, $^4J = 1.4$, H-C(5)); 6.41 (d, 2H, $^3J = 4.9$, H-C(4')). MS (electrospray) m/z : 605 (100, $\text{M} - \text{Cl}^-$). UV-vis (λ (nm), ϵ ($\text{M}^{-1} \text{cm}^{-1}$)) (CH_3CN): 374 (9600), 284 (29200). Anal. Calcd for $\text{C}_{28}\text{H}_{18}\text{N}_4\text{S}_2\text{RhCl} \cdot (\text{CH}_3\text{COOEt})_2 \cdot (\text{H}_2\text{O})_4$: C, 48.62%; H, 4.76%; N, 9.45%. Found: C, 48.74%; H, 4.30%; N, 9.34%.

Computational Details. All DFT and time-dependent DFT (TD-DFT) calculations reported in this paper were carried out using Gaussian 98.²⁰ The mPW1PW functional²¹ was used in all calculations. The 6-31G(d) basis set was employed for the ligands, and the SDD basis-set and effective core potential²² were used for rhodium. An unpruned Lebedev grid of 75 radial and 302 angular points was employed in all calculations. The ground state geometries of the complexes were optimized at the DFT level of theory employing the tight convergence criterion prior to the TD-DFT calculations of the triplet state energies. The geometries were constrained to C_2 symmetry during all of the calculations. The orbital pictures presented in this publication were generated using MOLEKEL 4.2.^{23,24}

(19) Maeder, U.; Von Zelewsky, A.; Stoeckli-Evans, H. *Helv. Chim. Acta* **1992**, *75*, 1320–1332.

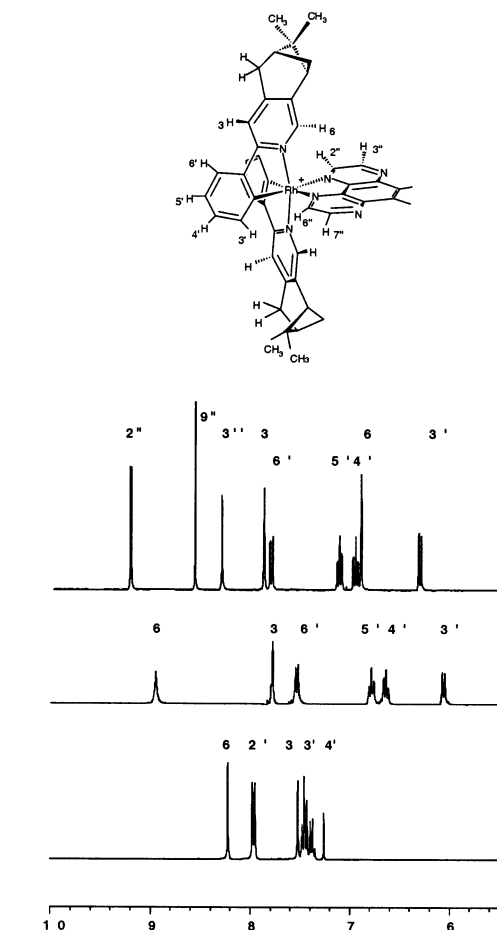


Figure 1. Aromatic region of the ^1H NMR spectra (300 MHz) of $\Delta[\text{Rh}(\text{phpy}4,5\text{p}(\text{R},\text{R})\text{py})_2\text{TAP}]\text{Cl}$ (top) in CD_3CN , $\Delta\Delta[\text{Rh}(\text{phpy}4,5\text{p}(\text{R},\text{R})\text{py})_2(\mu\text{-Cl})]_2$ (middle) in CD_3CN , and $\text{phpy}4,5\text{p}(\text{R},\text{R})\text{py}$ (bottom) in CD_3CN . For the numbering of the protons, see insert.

Results

^1H NMR Spectroscopy. The dinuclear complex ($\Delta\Delta\text{Rh}(\text{phpy})$) has D_2 symmetry, yielding only one set of ^1H NMR signals for the four ligands. The aromatic region of the ^1H NMR spectrum (Figure 1) shows only six signals, owing to the high symmetry of this species. The assignment of the protons was made by comparison with the already reported ($\text{Rh}(\text{Rh}(\text{phpy}))$) spectra¹⁵ (Figure 1). The signal

(20) Frisch, M. J.; Trucks, G. W.; Schlegel, H. B.; Scuseria, G. E.; Robb, M. A.; Cheeseman, J. R.; Zakrzewski, V. G.; Montgomery, J. A., Jr.; Stratmann, R. E.; Burant, J. C.; Dapprich, S.; Millam, J. M.; Daniels, A. D.; Kudin, K. N.; Strain, M. C.; Farkas, O.; Tomasi, J.; Barone, V.; Cossi, M.; Cammi, R.; Mennucci, B.; Pomelli, C.; Adamo, C.; Clifford, S.; Ochterski, J.; Petersson, G. A.; Ayala, P. Y.; Cui, Q.; Morokuma, K.; Malick, D. K.; Rabuck, A. D.; Raghavachari, K.; Foresman, J. B.; Cioslowski, J.; Ortiz, J. V.; Stefanov, B. B.; Liu, G.; Liashenko, A.; Piskorz, P.; Komaromi, I.; Gomperts, R.; Martin, R. L.; Fox, D. J.; Keith, T.; Al-Laham, M. A.; Peng, C. Y.; Nanayakkara, A.; Gonzalez, C.; Challacombe, M.; Gill, P. M. W.; Johnson, B. G.; Chen, W.; Wong, M. W.; Andres, J. L.; Head-Gordon, M.; Replogle, E. S.; Pople, J. A. *Gaussian 98*, revision A.7.M; Gaussian, Inc.: Pittsburgh, PA, 1998.

(21) Adamo, C.; Barone, V. *J. Chem. Phys.* **1998**, *108*, 664–675.

(22) Leininger, T.; Nicklass, A.; Stoll, H.; Dolg, M.; Schwerdtfeger, P. *J. Chem. Phys.* **1996**, *105*, 1052–1059.

(23) Portmann, S.; Lüthi, H. P. *Chimia* **2000**, *54*, 766–770.

(24) Flükiger, P.; Lüthi, H. P.; Portmann, S.; Weber, J. *MOLEKEL 4.2*; Swiss Center for Scientific Computing: Manno, Switzerland, 2002–2002.

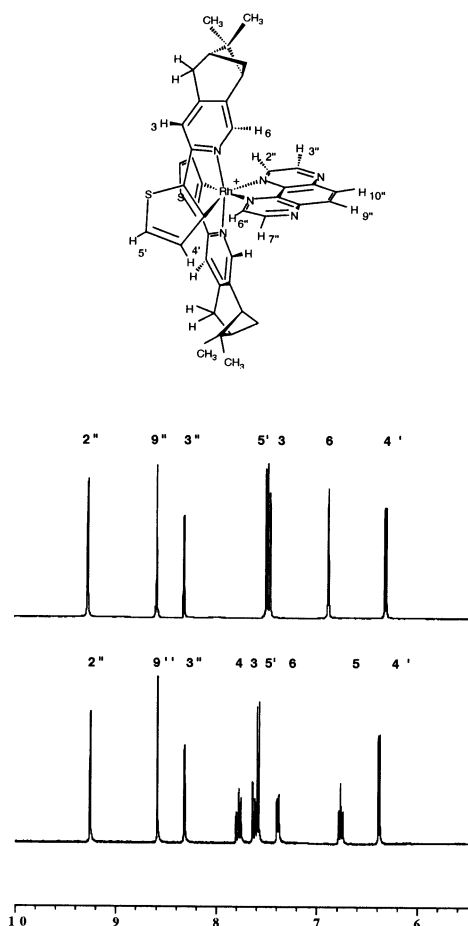


Figure 2. Aromatic region of the ^1H NMR spectra of $\Delta[\text{Rh}(\text{thpy}4,5\text{p}-(R,R)\text{py})_2\text{TAP}]\text{Cl}$ (top) in CD_3CN and $[\text{Rh}(\text{thpy})_2\text{TAP}]\text{Cl}$ (bottom) in CD_3CN . For the numbering of the protons, see insert.

corresponding to the proton $2'\text{-H}$ in the free ligand disappears indicating that the cyclometalation occurred.

All the mononuclear complexes have C_2 symmetry giving rise to one set of signals. Since they all contain the TAP ligand, the characteristics of this ligand are easily recognized in the ^1H NMR spectra (Figures 1 and 2). The three signals of the TAP always appear at lower field as compared to those of the cyclometalated ligands, due to the π -deficient character of the TAP. The assignment of the protons for the four mononuclear complexes has been performed by comparison with the signals previously reported for $\text{Rh}(\text{phpy})$.¹⁰

Absorption and CD Spectroscopy. The absorption bands that occur up to 340 nm are due to ligand centered ($\pi-\pi^*$) transitions.²⁵ In the broad intense bands of lower energy between 350 and 380 nm (see Experimental Section), a charge transfer (CT) contribution could be present since no absorptions are observed for the free ligands in this wavelength region.^{11,14}

The chiral bidentate ligands (8*R*,10*R*)-2-(2'-thienyl)-4,5-pinenopyridine, (8*S*,10*S*)-2-(2'-thienyl)-4,5-pinenopyridine, and (8*R*,10*R*)-2-(2'-phenyl)-4,5-pinenopyridine used for the preparation of the dinuclear Rh–Rh precursors show no easily detectable CD activity in the range 230–800 nm, while, upon cyclometalation to Rh(III), a strong Cotton effect

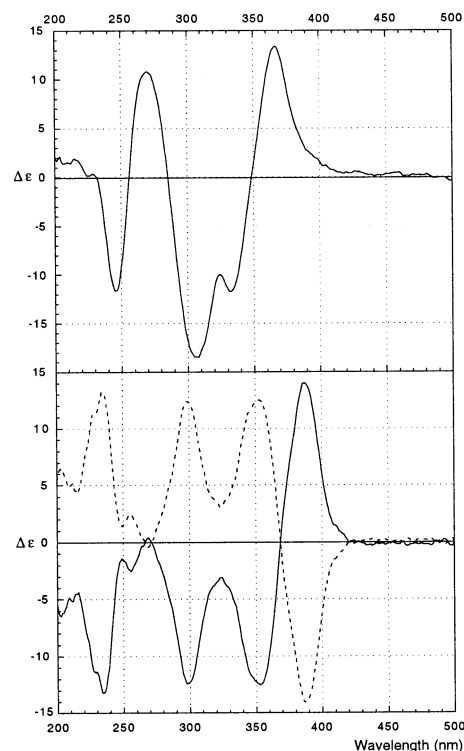


Figure 3. CD spectra in CH_3CN (molar CD, $\text{M}^{-1}\text{cm}^{-1}$) of $\Delta[\text{Rh}(\text{phpy}4,5\text{p}-(R,R)\text{py})_2\text{TAP}]\text{Cl}$ (—) (top) and the two enantiomers $\Delta[\text{Rh}(\text{thpy}4,5\text{p}-(R,R)\text{py})_2\text{TAP}]\text{Cl}$ (---) and $\Lambda[\text{Rh}(\text{thpy}4,5\text{p}-(S,S)\text{py})_2\text{TAP}]\text{Cl}$ (- - -) (bottom).

is observed. This indicates that, for the Rh–Rh complexes, the CD activity is mainly determined by the chiral configuration of the metal centers, and the activity of the “pineno” moieties is negligible.

The CD spectrum in acetonitrile of the $\Delta\Delta\text{Rh-Rh}(\text{phpy})$ dinuclear species shows a strong positive Cotton effect at 369 nm ($\Delta\epsilon = 6.6$), similar to the CD spectrum of $\Delta\Delta\text{Rh-Rh}(\text{thpy})$. Since for $\Delta\Delta\text{Rh-Rh}(\text{thpy})$ the exact configuration at the metal centers was previously¹³ confirmed by X-ray, the assignment of the absolute configuration of dinuclear complex Rh–Rh(phpy) to $\Delta\Delta$ is straightforward. This correlation can be applied because the orientation of the pinene groups (*R,R*) fused to the pyridine rings induces the same steric hindrance which leads to the same helical arrangement of the ligands around the metal centers.

The mononuclear complexes $\Delta\text{Rh}(\text{thpy})$ and $\Delta\text{Rh}(\text{phpy})$, obtained by cleavage reactions of the corresponding dinuclear precursors, exhibit a complete retention of configuration at the metal centers. Indeed, the CD spectra of $\Delta\text{Rh}(\text{thpy})$ and $\Delta\text{Rh}(\text{phpy})$ show the same strong positive Cotton effect at the longest absorption wavelength (Figure 3). Their CD spectra have the same shapes as those of the $\Delta\Delta$ precursors and the reported spectra of other optically active $\Delta[\text{Rh}(\text{thpy}4,5\text{p}-(R,R)\text{py})_2(\text{N}\wedge\text{N})]\text{Cl}$ complexes.¹⁴ Moreover, $\Delta\text{Rh}(\text{thpy})$ and $\Lambda\text{Rh}(\text{thpy})$ are enantiomers as well as they show mirror images in their CD spectra.

Emission Spectroscopy: With phpy as Cyclometalating Ligand. The corresponding dichloro-bridged dimer Rh–Rh(phpy) has been shown to exhibit a structure in its 77 K emission spectrum with an associated lifetime of 93 μs ; no

(25) Schumm, S.; Kirsch-De Mesmaeker, A. To be submitted.

Table 1. Emission Data for the Rh(III) Complexes^a

	298 K		77 K				
	$\lambda_{\max}/\text{nm}^b$	$\tau/\text{ns}^{b,g}$	$\lambda_{\max}/\text{nm}^c$	$\tau_1/\mu\text{s}^{c,h}$	E_1 in %	$\tau_{2/3} \pm \sigma_{2/3}/\mu\text{s}$	$E_{2/3}$ in %
[Rh(thpy) ₂ (μ -Cl)] ₂	<i>d</i>	<i>d</i>	533 ^e 553 577 600	270 270 270 270			
[Rh(thpy) ₂ TAP]Cl	695 (735) ^c	17 (<1) ^c	523 ^e 543 566	4.2 ± 1.2 ^f 6.7 ± 0.3 ^f 5.8 ± 0.1 ^f	1 8 12	72 ± 5 463 ± 7 23 ± 3 291 ± 4 25 ± 2 388 ± 18	6 93 12 80 8 80
Δ [Rh(thpy4,5p(<i>R,R</i>)) ₂ TAP]Cl	720 <i>d</i>	11 <i>d</i>	526 ^e 570 625 550	5.8 ± 0.5 ^f 3.6 ± 0.1 ^f 2.6 ± 0.1 ^f 8.4	4 31 24	15.3 ± 0.6 29 ± 3 272 ± 3 9.7 ± 0.5 7.9 ± 0.2	56 6 90 69 76
[Rh(phpy) ₂ TAP]Cl	635 (680) ^c	175 (40) ^c	550	8.4			
Δ [Rh(phpy4,5p(<i>R,R</i>)) ₂ TAP]Cl	647 (690) ^c	152 (32) ^c	553	9			
Hthpy ^{15,21}	<i>i</i>	<i>i</i>	486 ^{e,j}	35 ms			
Hphpy ^{15,21}	<i>i</i>	<i>i</i>	430 ^{e,j}	> 100 ms			

^a $\tau_{1/2/3}$, discrete lifetime components; $E_{1/2/3}$, relative preexponential factors. ^b In acetonitrile, if not mentioned otherwise. ^c In ethanol/methanol 4:1 mixture. ^d Slightly soluble in acetonitrile and alcoholic mixture, no emission detectable. ^e Structured emission with multiple emission maxima. ^f The shorter lifetime could not be determined correctly due to the presence of long lifetimes. Therefore, the shorter lifetime was determined during an independent measurement with a shorter time range. ^g Luminescence lifetime measurements using the SPC Edinburgh Instruments, see Experimental Section. ^h Luminescence lifetime measurements using the Nd:YAG laser equipment, see Experimental Section. ⁱ Not soluble in acetonitrile. ^j Highest energy feature of the emission band.

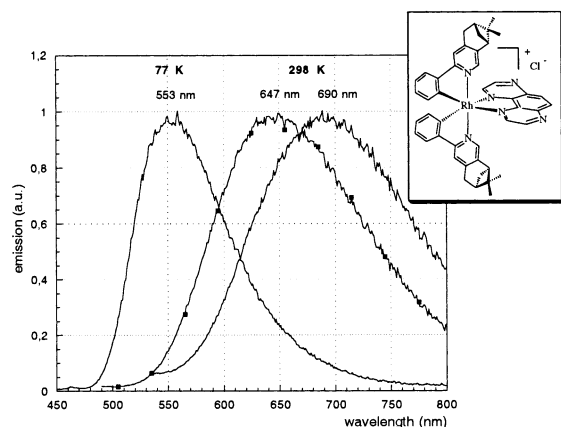


Figure 4. Emission spectra of Δ [Rh(phpy4,5p(*R,R*))₂TAP]Cl in acetonitrile (—■—) at 298 K and in an EtOH/MeOH 4:1 mixture (—○—) at 298 and 77 K.

emission was detected at room temperature.¹⁵ These data and similarities with the spectrum at 77 K of the free “protonated” ligand indicated that the luminescence originates from a ³LC state.^{11,15} Comparison of these emission data for Rh–Rh(phpy) with those of the mononuclear species Rh(phpy) stresses the important difference between the two complexes. The spectrum of the mononuclear Rh(phpy) compound at 77 K is indeed structureless with a shorter associated lifetime of 8.4 μs ; moreover, a structureless emission is also recorded in acetonitrile and in [EtOH/MeOH] 4:1 at room temperature with associated lifetimes of 175 and 40 ns, respectively, (Table 1). This ensemble of data is clearly characteristic of CT emissions.

The new complex Δ Rh(phpy) shows globally the same characteristic emission features (Figure 4 and Table 1). Comparison of the emissions of Δ Rh(phpy) with those of Rh(phpy) indicates only a slight red shift of the optically

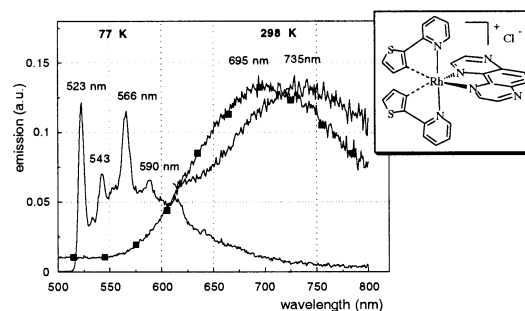


Figure 5. Emission spectra of [Rh(thpy)₂TAP]Cl in acetonitrile (—■—) at 298 K and in an EtOH/MeOH 4:1 mixture (—○—) at 298 and 77 K.

pure complex at room temperature. The luminescence lifetimes are 9 μs at 77 K, whereas at room temperature values of 152 ns were measured in acetonitrile and 32 ns in [EtOH/MeOH] 4:1.

With thpy as Cyclometalating Ligand. The dinuclear complex Rh–Rh(thpy) emits at 77 K in an alcoholic matrix ([EtOH/MeOH] 4:1) with a highly structured spectrum, and the luminescence decay corresponds to a single exponential with a long lifetime of 270 μs at different wavelengths (Table 1). This complex does not emit at room temperature, neither in acetonitrile nor in the alcoholic mixture. The mononuclear species Rh(thpy), like its precursor Rh–Rh(thpy), exhibits a highly structured luminescence at 77 K (Figure 5). The emission maxima are only slightly blue shifted by approximately 10 nm as compared to the dinuclear precursor. This behavior is thus different from that of the emission spectra at 77 K of Rh(phpy). Moreover, in contrast to Rh(phpy), the luminescence lifetimes of Rh(thpy) depend on the emission wavelength, and the decays do not correspond to single exponentials but multiexponentials. The lifetimes and relative preexponential factors of each component at the

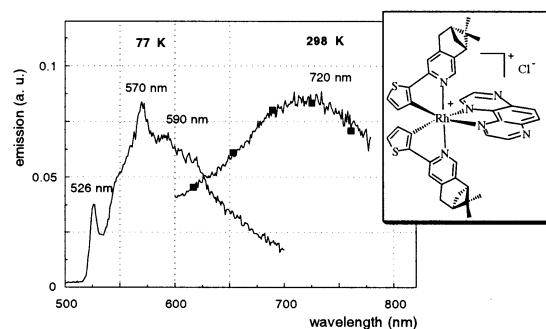


Figure 6. Emission spectra of Δ [Rh(thpy)₄,5p(R,R)py)₂TAP]Cl in acetonitrile (—■—) at 298 K and in an EtOH/MeOH 4:1 mixture (—) at 77 K.

different wavelengths are collected in Table 1. From shorter to longer wavelengths, the contribution of the longer lifetime component becomes vanishingly small. We have to note that these decays and their analyses corresponding to a triexponential, have not the same quality as those at 298 K that are single exponentials. Indeed, at 77 K, the whole decay is registered after a single laser pulse. Moreover, it cannot be analyzed within one single time window which complicates very much the analysis. In contrast, at 298 K, the decay curve is measured by a sampling method, i.e., single photon counting, and can be analyzed within the same time window. Consequently, the values of $\tau_{1/2/3}$ and $E_{1/2/3}$ in Table 1 from the multiexponential decays analyses at 77 K should be regarded with caution. Nevertheless, the analyses indicate clearly the presence of three lifetimes: a few microseconds, a few tens of microseconds, and a few hundreds of microseconds.

At room temperature, the emission spectra of Rh(thpy) (Figure 5) are structureless in both acetonitrile and alcoholic mixture. The emission maximum is red shifted compared to that of the phpy complex. The corresponding luminescence decays under pulsed illumination are single exponentials (Table 1).

The emission properties of Δ Rh(thpy) are of course identical to those of Λ Rh(thpy) as they are enantiomers; therefore, in the discussion, only Δ Rh(thpy) will be considered. The attachment of the pinene group to the thpy ligand has only a slight effect on the emission at room temperature or at 77 K (Figure 6). In the solvent matrix at 77 K, the emission spectrum is broader and somewhat less structured than that of Rh(thpy). The corresponding luminescence decays are similar to those of Rh(thpy) and do not correspond to single exponentials at 77 K (Table 1). At room temperature, the emission maximum of Δ Rh(thpy) in acetonitrile is slightly red shifted compared to that of Rh(thpy), and no emission was observed in alcoholic mixture ([EtOH/MeOH] 4:1).

TD-DFT Calculations for the Triplet Excited States of Rh(phpy) and Rh(thpy). In the TD-DFT approach, the excited states are calculated in terms of particle–hole (excitations) and hole–particle (de-excitation) amplitudes with respect to the ground state DFT wave function.^{26–29} Each electronic state calculated in this way can then be assigned according to the nature of the orbitals involved in the principal excitations (most important configurations) for

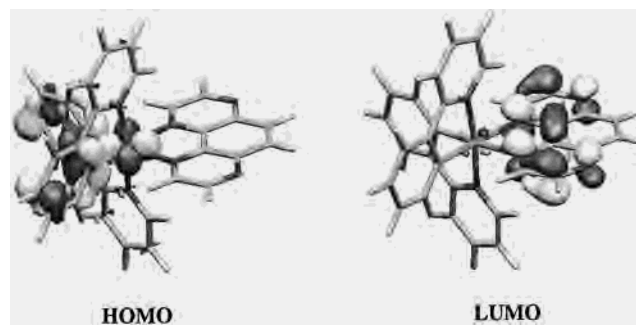


Figure 7. Frontier orbitals of [Rh(phpy)₂TAP]⁺.

Table 2. Orbitals Involved in the Description of the Seven Lowest Triplet States of [Rh(phpy)₂TAP]⁺ and [Rh(thpy)₂TAP]⁺

[Rh(phpy) ₂ TAP] ⁺			[Rh(thpy) ₂ TAP] ⁺		
orbital	contribution	name	orbital	contribution	name
LUMO + 3	7% d _{Rh} 91% π _{phpy} 2% π _{TAP}	L ₃	LUMO + 3	8% d _{Rh} 89% π _{thpy} 3% π _{TAP}	L ₃
LUMO + 2	7% d _{Rh} 88% π _{phpy} 5% π _{TAP}	L ₂	LUMO + 2	9% d _{Rh} 86% π _{thpy} 5% π _{TAP}	L ₂
LUMO + 1	1% d _{Rh} 1% π _{phpy} 98% π _{TAP}	L ₁	LUMO + 1	1% d _{Rh} 1% π _{thpy} 98% π _{TAP}	L ₁
LUMO	5% d _{Rh} 2% π _{phpy} 93% π _{TAP}	L ₀	LUMO	5% d _{Rh} 2% π _{thpy} 93% π _{TAP}	L ₀
HOMO	40% d _{Rh} 58% π _{phpy} 2% π _{TAP}	H ₀	HOMO	24% d _{Rh} 74% π _{thpy} 2% π _{TAP}	H ₀
HOMO – 1	3% d _{Rh} 95% π _{phpy} 2% π _{TAP}	H ₁	HOMO – 1	2% d _{Rh} 97% π _{thpy} 1% π _{TAP}	H ₁
HOMO – 2	9% d _{Rh} 90% π _{phpy} 1% π _{TAP}	H ₂	HOMO – 5	71% d _{Rh} 19% π _{thpy} 10% π _{TAP}	H ₅
HOMO – 7	10% d _{Rh} 14% π _{phpy} 76% π _{TAP}	H ₇	HOMO – 6	6% d _{Rh} 7% π _{thpy} 87% π _{TAP}	H ₆
HOMO – 8	1% d _{Rh} 3% π _{phpy} 96% π _{TAP}	H ₈			

the respective state. The most important orbitals for the description of the first seven triplet states of Rh(phpy) and Rh(thpy) are listed in Table 2. The spectroscopic properties of transition-metal complexes are usually discussed in terms of localized molecular orbitals and are thus classified as metal-centered (MC), ligand-centered (LC), or metal-to-ligand charge-transfer (MLCT), assuming a more or less pure character of the orbitals involved in the respective excitations. In this context, it is interesting to note that for both complexes considered here the HOMO has a mixed character, being partly localized on the central metal and partly on the cyclometalating ligand (Figure 7). This is in agreement with a recent TD-DFT study on iridium complexes containing the phpy ligand.³⁰ Furthermore, it is mentioned in the literature^{31–33}

(26) Jamorski, C.; Casida, M. E.; Salahub, D. R. *J. Chem. Phys.* **1996**, *104*, 5134–5147.

(27) Stratmann, R. E.; Scuseria, G. E.; Frisch, M. J. *J. Chem. Phys.* **1998**, *109*, 8218–8224.

(28) Casida, M. E. *J. Chem. Phys.* **1998**, *108*, 4439–4449.

(29) Bauernschmitt, R.; Ahlrichs, R.; Hennrich, F. H.; Kappes, M. M. *J. Am. Chem. Soc.* **1998**, *120*, 5052–5059.

(30) Hay, P. J. *J. Phys. Chem. A* **2002**, *106*, 1634–1641.

that, due to the high degree of covalency of the C⁻–Rh bonds, a description of the electronic structure in terms of orbitals localized on either the central metal or the ligands is not sufficient. The largest contribution to the HOMO is in both cases from the π -orbitals of the cyclometalating ligand; however, there is a considerable mixing with the d-orbitals of rhodium which amounts to 40% metal character in the case of the phpy complex and 24% for the thpy complex (Table 2, Figure 7). The remaining molecular orbitals listed in Table 2 (HOMO or LUMO) can be regarded as localized at either the different types of ligands or the central metal atom with only minor degrees of orbital mixing. Table 3a,b lists the calculated energies of the seven lowest triplet states of Rh(phpy) and Rh(thpy), respectively. The character of the different states has been assigned according to the principal orbital substitutions (excitations) as determined from the TD-DFT calculations (cf. column 4 in Tables 3a and 3b). Due to the orbital mixing observed for the HOMO, the lowest triplet state (T₁) has in both cases the character of a ligand-to-ligand charge-transfer state (LLCT) from cyclometalated ligand (thpy or phpy) to the TAP ligand, with some admixture of MLCT character. This is in contrast to previous assignments of these states as purely MLCT or SBLCT (single-bond-to-ligand CT).¹⁰

Discussion and Conclusions

The results of this work demonstrate clearly that Δ Rh(thpy), Δ Rh(phpy), and Δ Rh(phpy) can be prepared and purified. After a careful checking of their purity by HPLC, they have been characterized by NMR and mass and CD spectroscopy. They can thus be tested in the future as DNA photoprobes. The thpy and phpy Rh(III) complexes with the TAP ligand show, rather unexpectedly, different absorption–emission behaviors. These properties could also be exploited advantageously for reporting interaction of the probe with DNA. In the following, we discuss the photophysical differences between the complexes. The emission behaviors are rationalized from the results of TD-DFT calculations for the triplet excited states.

Absorption. The UV absorption spectra of the “protonated” ligands Hthpy¹³ and Hphpy¹⁰ and the π accepting TAP ligand (not soluble in CH₃CN; $\lambda_{\text{max}} = 280$ nm, $\epsilon = 27000$ M⁻¹ cm⁻¹ in EtOH/MeOH 4:1) show intense ultraviolet absorption bands in the 240–320 nm region; the most bathochromic absorption is found for Hthpy (Hthpy, $\lambda_{\text{max}} = 302$ nm; Hphpy, $\lambda_{\text{max}} = 247$ nm in CH₃CN). The spectra of the corresponding Rh(III) complexes display also high-intensity UV bands; however, their comparison with those of the corresponding free ligands does not allow clear assignments of the bands of the complexes to the specific ligands although this can generally be done with the Ru(II) complexes. As the cyclometalating ligands have lost a proton

in the complex, they should indeed not exhibit the same π – π^* transitions.

Although for the mononuclear complexes Rh(thpy), Δ Rh(thpy), and Δ Rh(phpy), we cannot assign, in a straightforward way, the absorption bands in the 374–380 nm region to LC transitions, these bands can certainly not be assigned to metal centered (MC) transitions. Indeed, this would not be compatible with their high intensity of absorption. Moreover because thpy (and its pinene derivative) has a relatively high ligand field strength, one would not expect an MC transition at such a low energy.^{11,16} On the other hand, comparison of the absorption spectra of the thpy mononuclear species with those of the dinuclear precursors Rh–Rh(thpy) and $\Delta\Delta$ Rh–Rh(thpy) shows that similar intense absorption bands are present. Since there is no TAP ligand in these dinuclear complexes, the transitions should involve the thpy ligands. However, for the mononuclear complex, an additional contribution from a CT toward the TAP ligand cannot be excluded.

For the 352–359 nm absorptions of Rh(phpy) and Δ Rh(phpy), as compared to the absorptions of the dinuclear species, the same type of conclusion as for the corresponding (thpy) complexes can be made. Thus, the most bathochromic absorption would involve the (phpy) ligand. In agreement with this, the absorptions of the phpy complexes are indeed more hypsochromic than those for the thpy complexes, as expected from the absorption of the free “protonated” ligands Hphpy and Hthpy.

Assignment of the Emission for Rh(thpy) and Rh(phpy), thpy Complexes at 77 K. The emission of the dinuclear complex Rh–Rh(thpy) recorded at 77 K is highly structured and decays monoexponentially with a relatively long excited state lifetime (270 μ s) (Table 1), which is typical for a ³LC π – π^* emission. The intensity pattern observed for the mononuclear Rh(thpy) complex at 77 K (Figure 5) looks strikingly similar to that of the dinuclear Rh–Rh(thpy) complex, with the emission maxima of the fine structure only slightly blue shifted (Table 1). This indicates that the electronic states responsible for the structured emission are of the same nature in both complexes and are most likely to be assigned to ³LC π – π^* states localized on the thpy ligands. However, in contrast to the dinuclear Rh–Rh(thpy) complex with its monoexponential decay, a multiexponential emission was found for the mononuclear Rh(thpy) complex. On the basis of the recorded NMR and ESMS spectra as well as the HPLC analyses, we are confident that impurities can be ruled out as sources for the multiexponential decay. Thus, several thermally nonequilibrated states are supposed to contribute to the emission of the mononuclear Rh(thpy) complex at 77 K. Interestingly, the relative contributions of the long and short lifetime components to the emission decay depend strongly on the wavelength. On the basis of the TD-DFT calculations, different triplets could be possible candidates for these different contributions. Among them, only the calculated triplets with energies in the range detected in emission will be considered. At 523 nm (2.37 eV), the emission is dominated by the long lifetime component ($\tau_3 = 463$ μ s, 93%), which is associated with a ³LC π – π^* emission

(31) Sandrini, D.; Maestri, M.; Ciano, M.; Maeder, U.; von Zelewsky, A. *Helv. Chim. Acta* **1990**, *73*, 1306–1313.

(32) Sandrini, D.; Maestri, M.; Balzani, V.; Maeder, U.; von Zelewsky, A. *Inorg. Chem.* **1988**, *27*, 2640–2643.

(33) Zilian, A.; Maeder, U.; von Zelewski, A.; Güdel, H. U. *J. Am. Chem. Soc.* **1989**, *111*, 3855–3859.

Table 3. Calculated Triplet State Energies and Assignment According to the Character of the Orbitals Involved for [Rh(phpy)₂TAP]⁺ and [Rh(thpy)₂TAP]⁺

state	energy (eV)	principal excitations	assignment
a. [Rh(phpy) ₂ TAP] ⁺			
T ₁	2.30	H ₀ → L ₀	LLCT($\pi_{\text{phpy}} \rightarrow \pi^*_{\text{TAP}}$)
T ₂	2.55	H ₀ → L ₁	LLCT($\pi_{\text{phpy}} \rightarrow \pi^*_{\text{TAP}}$)
T ₃	2.63	H ₇ → L ₁	LC $\pi\pi^*$ (TAP)
		H ₈ → L ₁	
T ₄	2.77	H ₁ → L ₃	LC $\pi\pi^*$ (phpy)
		H ₀ → L ₂	
T ₅	2.78	H ₁ → L ₂	LC $\pi\pi^*$ (phpy)
		H ₀ → L ₃	
T ₆	2.82	H ₁ → L ₀	LLCT($\pi_{\text{phpy}} \rightarrow \pi^*_{\text{TAP}}$)
T ₇	3.02	H ₂ → L ₀	LLCT($\pi_{\text{phpy}} \rightarrow \pi^*_{\text{TAP}}$)
		H ₁ → L ₁	
b. [Rh(thpy) ₂ TAP] ⁺			
T ₁	2.14	H ₀ → L ₀	LLCT($\pi_{\text{thpy}} \rightarrow \pi^*_{\text{TAP}}$)
T ₂	2.36	H ₀ → L ₁	LLCT($\pi_{\text{thpy}} \rightarrow \pi^*_{\text{TAP}}$)
		H ₁ → L ₂	+ LC $\pi\pi^*$ (thpy)
		H ₀ → L ₃	
T ₃	2.39	H ₀ → L ₂	LC $\pi\pi^*$ (thpy)
		H ₁ → L ₃	
T ₄	2.41	H ₀ → L ₃	LC $\pi\pi^*$ (thpy)
		H ₁ → L ₂	+ LLCT($\pi_{\text{thpy}} \rightarrow \pi^*_{\text{TAP}}$)
		H ₁ → L ₀	
T ₅	2.49	H ₁ → L ₀	LLCT($\pi_{\text{thpy}} \rightarrow \pi^*_{\text{TAP}}$)
		H ₀ → L ₁	
T ₆	2.63	H ₆ → L ₁	LC $\pi\pi^*$ (TAP)
		H ₅ → L ₁	+MLCT(TAP)
T ₇	2.68	H ₁ → L ₁	LLCT $\pi\pi^*$ ($\pi_{\text{thpy}} \rightarrow \pi^*_{\text{TAP}}$)

that is responsible for the observed structure. This is in surprisingly good agreement with the excitation energy of 2.41–2.36 eV calculated for the triplet T₄, T₃, and T₂ states where only T₃ corresponds to a pure LC $\pi\pi^*$ state localized on the thpy ligands (Table 3b). At longer wavelengths, the short lifetime component gets more and more important and finally dominates the emission from 590 nm (2.10 eV). This short lifetime component is missing in the spectrum of the dinuclear complex. Since the main difference between the mononuclear and the dinuclear complex is the presence of the TAP ligand, it seems reasonable to assume that the TAP ligand is involved in the excited states that lead to the additional emission component at 590 nm observed for the mononuclear Rh(thpy) complex. Indeed, the lifetime τ_1 , which is on the order of a few microseconds, is quite characteristic for a pure ³CT state and could originate from T₁ (2.14 eV, Table 3b). The second lifetime τ_2 , which is roughly 1 order of magnitude larger than τ_1 , is unusually long to be assigned to a pure ³CT state and too short for a pure ³LC state. Therefore, the calculated T₂ at 2.36 eV or T₄ at 2.41 eV from the TD-DFT calculations could be responsible for these emissions (Table 3b) because they originate from states with a mixed CT and LC character.

thpy Complexes at 298 K. At room temperature (under air or argon), no emission was observed for Rh–Rh(thpy) in acetonitrile. This is in agreement with the fact that ³LC $\pi\pi^*$ states are expected to be efficiently quenched in solution due to their long lifetime. In contrast to this, a structureless emission was detected (Figure 5) for the mononuclear Rh(thpy) complex at 298 K. This emission decays monoexponentially with a lifetime in the nanosecond time scale (1–17 ns). Furthermore, the emission band is strongly shifted

to lower energies compared to the spectra at 77 K, and the magnitude of the spectral shift depends on the polarity of the solvent (Table 1). Thus, the emission shows the characteristics of a charge transfer (CT) state. This observation is consistent with the lowest triplet state of the mononuclear Rh(thpy) complex being a ³LLCT state involving the TAP ligand as predicted by the TD-DFT calculations. No ³LC $\pi\pi^*$ (thpy) emission is detectable at room temperature for this mononuclear compound as observed for the corresponding dinuclear complex where the lowest excited state is a LC $\pi\pi^*$ (thpy) triplet.

Optically Active thpy Complexes. The emission properties of Δ Rh(thpy) are very similar to those of the structurally related Rh(thpy) (Table 1). Therefore, it is reasonable to consider the same assignment for the emission of Δ Rh(thpy). The fact that the low temperature emission spectrum is less structured (Figure 6) than that of Rh(thpy) is probably due to the fusion of the pinene to the pyridine part of the ligand, which may alter the vibrational energy structure of the thpy ligand and also have a slight influence on the electronic properties.

Phpy Complexes. Structureless emission bands were recorded for Rh(phpy) both at room temperature and at 77 K in a solid matrix (Table 1). The emission maximum at 298 K is strongly shifted to longer wavelengths compared to the low temperature spectrum, and the magnitude of the spectral shift is solvent dependent (Table 1). Furthermore, the emission decays monoexponentially with a lifetime that is characteristic for a ³CT state at both temperatures. The TD-DFT calculations predict the lowest triplet state of Rh(phpy) to be of LLCT character (Table 3a) involving an excitation from the mainly phpy centered HOMO to the TAP centered LUMO which is in agreement with the above-mentioned observations.

It is important to note that the calculated excitation energy of the T₁ state (2.30 eV) is very close to the energy of the emission maximum recorded at 77 K thus in the absence of solvent relaxation (2.25 eV). The emission properties of Δ Rh(phpy) are again very similar to those of the structurally related Rh(phpy) (Figure 4, Table 1), and thus, it seems to be justified to assign the emission of Δ Rh(phpy) to a ³LLCT as well.

Comparison between the thpy and phpy Complexes. It is quite surprising that, for Rh(phpy), only one LLCT (T₁) state emits at 77 K whereas more than one state and a structured emission are detected for the thpy complexes at low temperature. The competition between the emission from the higher triplet states and the nonradiative decay from these states to the T₁ state should be governed by different factors. It has been observed by Watts et al.^{34,35} for a number of transition-metal complexes that the rate of nonradiative decay depends on the orbital parentage of the excited states involved. Thus, a nonradiative transition between states of the same orbital parentage (e.g., two CT states) should be

(34) Watts, R. J. *J. Am. Chem. Soc.* **1974**, *96*, 6186–6187.(35) Watts, R. J.; Brown, M. J.; Griffith, B. G.; Harrington, J. S. *J. Am. Chem. Soc.* **1975**, *97*, 6029–6036.

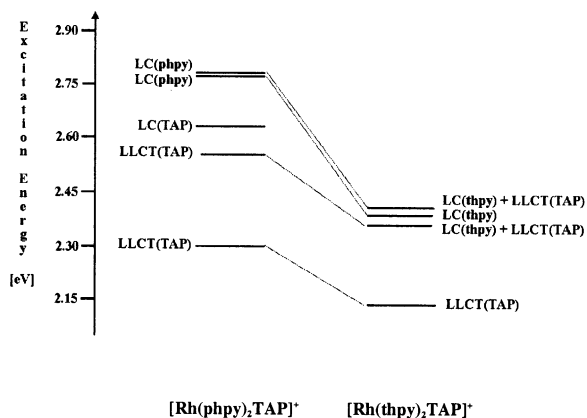


Figure 8. Energy levels of the first four triplets for Rh(phpy) and Rh(thpy).

faster than the transition between states of different orbital parentage (e.g., between a CT and a LC state). Furthermore, since nonradiative decay takes place between isoenergetic vibronic levels of the different electronic states, the efficiency of the process should depend on the energy difference (and relative displacement) between the electronic states. At small energy differences, the density of vibronic states, and thus the number of available decay channels, might be too limited to ensure efficient nonradiative decay. Thus, the energy differences between the states and the different orbital parentage could affect the decay process at 77 K.

As indicated in Table 3a,b and in Figure 8, the energy differences between the first four triplets are larger in Rh(phpy) than in Rh(thpy). Thus, according to this energy parameter, the nonradiative transitions from T_4 to T_3 , T_2 , and T_1 could be favored in Rh(phpy) compared to Rh(thpy). Moreover, considering the orbital parentage, the radiationless decays from T_4 to T_3 and T_2 to T_1 should also be favored in Rh(phpy) as compared to Rh(thpy). Indeed, whereas T_4 and T_3 have the same orbital parentage as well as T_2 and T_1 in Rh(phpy), this is not the case for the corresponding pairs of triplets (T_4 – T_3 and T_2 – T_1) in Rh(thpy).

On the other hand, it is also probable that other parameters than the energy differences or orbital parentages would play a role. As the crossing from one state to the other could also be regarded as an intramolecular electron (or charge) transfer process,³⁶ the parameters that control the rate constant of electron transfer could also influence the decays. Thus, the electron transfer process, for example, for the transition from T_3 to T_2 in Rh(phpy) and in Rh(thpy), could be kinetically different. Indeed, although in both complexes the decay concerns a transition from an LC state to a CT state (CT from the orthometalated to the TAP ligand), in Rh(phpy) the LC state is localized on the TAP whereas, in Rh(thpy), the LC state is localized on the orthometalated ligand. Thus, a different electron transfer process is implied for the transition $LC_{\pi-\pi^*}(T_3)$ to $CT(T_2)$ in the two complexes.

In conclusion, the inspection of the results of DFT calculations, in addition to considerations of the different factors that influence the transitions between the triplets, may explain the different photophysical behavior observed for the two Rh–TAP complexes.

Two novel optically pure Rh(III) complexes with a TAP ligand and pinene substituents on the ancillary phenylpyridine or thienylpyridine ligands have been prepared and characterized. Their photophysical properties are compared to the racemic forms without pinene. The different photophysics, associated to the two types of ancillary ligands, is discussed on the basis of TD-DFT calculations.

Acknowledgment. The authors wish to thank Didier Lötscher and Alex von Zelewsky for kindly providing the (1-phenacyl)pyridinium bromide, Guy Vandenbusche for the access to the CD spectrometer, Alain Van Dorsselaer for the ESMS measurements, and the PAI-IUAP 4/11 program for financial support. S.S. and O.L. thank, respectively, the TMR network (ERBFM-RXCT980226) and the FRIA for a fellowship. The COST D14 is also acknowledged.

IC020435I

(36) Pourtois, G.; Beljonne, D.; Lazzaroni, R.; Bredas, J. L.; Schumm, S.; Moucheron, C.; Kirsch-De Mesmaeker, A. To be submitted.